

Numerical Study Of Laminar Natural Convection In A Half Ellipsoid Of Revolution Subjected To Heat Flux Of Constant Density

Jaona Ramiaramananjafy¹, Ravaka Randriamorasata¹, Josoa Randriamorasata¹, François Ravalison^{1,2}

¹ University of Antananarivo

² Centre National de Recherches Industrielle et Technologique-CNRI
Antananarivo, Madagascar



Abstract— In this article, we numerically study the natural convection in a half-ellipsoid of revolution filled with a Newtonian fluid (air). The ellipsoid wall is isothermal which is maintained at a heat flux of constant density. The equations that govern the flow and heat transfer are described by the so-called Navier-Stokes equation of motion accompanied by the so-called Fourier equation of heat. The finite element method is used to solve the system of equations. We consider the effect of the shape factor of the elliptical wall and the Grashof number on the results obtained in the form of streamlines, and mean Nusselt numbers. The Nusselt numbers for natural convection inside a system formed by a rectangular geometry and for a curved shape are compared and analyzed each other. We find that this number is quite higher for a curved system than that of a planar shape. It shows the importance of the form factor, particularly, in circular shape which is much more advantageous compared to the straight shape.

In terms of inertia, the geometry of rounded shape ensures the best distribution of energy. In fact, the half ellipsoidal greenhouse with a circular base studied during this research offers a better distribution for the flow of the convection currents from the bottom to the top of the system.

Keywords— Thermo Convective/ Closed Enclosure/ Thermal Mass/ Thermal Inertia/Form Factor.

I. INTRODUCTION

Many studies have been conducted on natural convection. Currently this study covers a wide range leading to many results including natural convection (natural convection or forced convection). In addition, researchers have focused the study of natural convection on the geometry of a system: rectangular [4], square [1], cylindrical [3], spherical [5] and elliptical [7]. These studies have made it possible to model the phenomenon of convection, to analyze the influence of various parameters for specific applications such as dryers [14], greenhouses [15]The study of convection on a new type of geometry allows it to highlight the conditions guaranteeing the establishment of a laminar natural convection inside a given enclosure. The originality of this thesis is based on the study of the laminar natural convection, constituted by a semi-ellipsoidal geometric surface. This research focuses on the study of the evolution of the convective current, under the effect of heat flux of constant density, which will make it possible to characterize the temperature stability, to determine the physical parameters which influence the flow of the air inside the enclosure, ensuring the good condition of the crops in the greenhouse.

II. MATERIAL AND METHODS

A. Design Procedure: Mathematical Formulation Of The Problem

A.1. Position of the problem and simplifying assumptions

The study focuses on the flow of an incompressible Newtonian fluid in half ellipsoid subjected to a uniform heat flux density Figure 1. At time t_0 the temperature of the fluid inside the enclosure is uniform and equals T_0 . The solid wall forming the containment then undergoes a uniform density of heat flux Q . the following assumptions are made: the fluid is incompressible and the convection inside the enclosure is laminar. The physical properties of the fluid are constant, except for its density in the equation of motion, which is linearized as a function of temperature according to the Boussinesq approximation.

$$\rho = \rho_0[1 - \beta(T - T_0)] \quad (1)$$

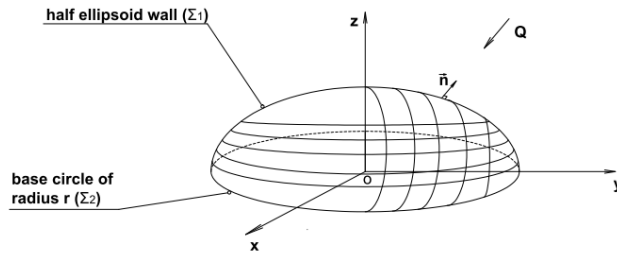


Figure 1: ellipsoidal surface subjected to a heat flux of constant density Q

A.2. Thermoconvective equations

In this study, the considered fluid is the air, the studied problem relates to a Thermoconvective phenomenon and governed by the following equations:

- The movement is described by the Navier-Stokes equations [10] to which we add the Boussinesq hypothesis.

$$\frac{\partial \vec{v}}{\partial t} + (\vec{v} \cdot \overrightarrow{\text{grad}}) \vec{v} = -\frac{1}{\rho} \overrightarrow{\text{grad}} p + \nu \Delta \vec{v} - \beta(T - T_0) \vec{g} \quad \text{in } \Omega \quad (2)$$

- The incompressibility of the fluid results in the continuity equation [10].

$$\text{div } \vec{v} = 0 \quad (3)$$

- The thermal convection [9], inside the domain is written by the Fourier equation.

$$\frac{\partial T}{\partial t} + \vec{v} \cdot \overrightarrow{\text{grad}} T = a \cdot \nabla^2 T \quad \text{within} \quad a = \frac{\lambda}{\rho \cdot c_p} \quad \text{in } \Omega \quad (4)$$

A.3. Initial conditions and boundary conditions

a- Initial conditions.

$$\text{At the moment :} \quad t_0 = 0 \quad \text{and} \quad v = 0 \quad (5)$$

$$\text{Furthermore:} \quad p = p_0 \quad \text{and} \quad T = T_0 \quad (6)$$

b- Boundary conditions

$$\text{The wall [11] comprises two parts } \Sigma_1 \text{ and } \Sigma_2 \text{ of which } \partial\Omega = \Sigma_1 \cup \Sigma_2 \quad (7)$$

where Σ_1 is formed by the surface of a semi-ellipsoid of revolution of equation

$$\left(\frac{x}{D}\right)^2 + \left(\frac{y}{D}\right)^2 + \left(\frac{z}{h}\right)^2 = 1 \quad (8)$$

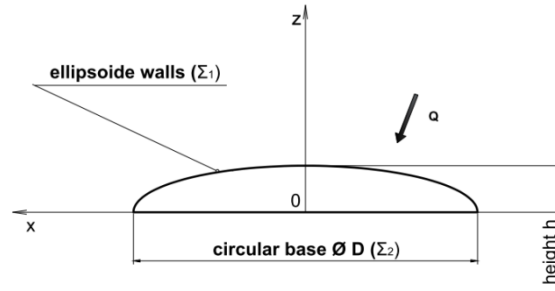


Figure 2: half-ellipsoid cut along the plane (0,x,z) subjected to a heat density Q

Σ_2 is the air-ground interface circular base (Figure 2) with equation:

$$\begin{cases} y = 0 \\ x^2 + z^2 \leq r^2 \end{cases} \quad (9)$$

So the boundary conditions are as follows:

. On the wall: $\partial\Omega = \Sigma_1 \cup \Sigma_2$; we have: $\vec{v} = 0$ (10)

. On Σ_2 ; the temperature is uniform: $T = Cte$ $T = T_0$ (11)

. On Σ_1 : $Q \cdot \vec{n} = -\lambda_p \cdot \overrightarrow{\text{grad}} T \cdot \vec{n}$ (12)

B. Numerical Resolution

To numerically solve the equations above [8], [13], we adopted the finite element methods and for the decoupling of the unknowns we used an Uzawa type method.

B.1. Adimensionnalization of the equations

We note l, v_0, t_0 et T_0 respectively the length, the velocity, the characteristic time of diffusion as well as the reference temperature and we note x^*, y^*, v^*, t^* and T^* the quantities dimensions defined by:

$$x^* = \frac{x}{l} ; y^* = \frac{y}{l} ; \vec{v}^* = \frac{\vec{v}}{v_0} ; t^* = \frac{t}{t_0} \text{ and } T^* = \frac{T}{T_0} \quad (13)$$

The dimensionless equations are then written

. Equation of motion

$$\frac{\partial \vec{v}^*}{\partial t^*} + (\vec{v}^* \cdot \nabla) \vec{v}^* = -\nabla p^* + \frac{1}{Re} \Delta \vec{v}^* - Gr(T^* - 1) \vec{e}_z \quad (14)$$

. Continuity equation

$$\text{div } \vec{v}^* = 0 \quad (15)$$

. Heat equation

$$\frac{\partial T^*}{\partial t^*} + \vec{v}^* \cdot \nabla T^* = \frac{1}{Pr} \Delta T^* \quad (16)$$

B.2. Initial conditions and boundary conditions [11].

With the boundary conditions:

$$. v^* = 0 \text{ on the walls} \quad \partial\Omega = \Sigma_1 \cup \Sigma_2 \quad (17)$$

$$. T^* = T_0 \text{ on } \Sigma_2 \quad (18)$$

$$. \frac{\partial T^*}{\partial \nu} = \frac{\nu^2}{g\beta T_0 l^5} Gr \text{ on } \Sigma_1 \quad (19)$$

Where Re , Gr and Pr denote respectively the dimensionless numbers of Reynolds, Grashof and Prandtl. They are defined by:

$$Re = \frac{v_0 l}{\nu} ; \quad Gr = \frac{g\beta l^4}{\lambda \nu^2} Q ; \quad Pr = \frac{\nu}{\alpha} = \frac{\rho \cdot C_p}{\lambda} \nu \quad (20)$$

C. Numerical Modeling

The discretization in time is done by finite differences. Thus we have the following explicit scheme knowing \vec{v}^*_n, T^*_n et p^*_n at time $t = n \cdot \delta\tau$ avec ($n \geq 0$), $\delta\tau$ is the time step, we calculate $\vec{v}^*_{n+1}, T^*_{n+1}$ et p^*_{n+1} which are solutions of:

$$\frac{\vec{v}^*_{n+1} - \vec{v}^*_n}{\delta\tau} - \frac{1}{Re} \Delta \vec{v}^*_{n+1} + (\vec{v}^*_{n+1} \cdot \vec{\nabla}) \vec{v}^*_{n+1} = -\vec{\nabla} p^*_{n+1} - Gr \vec{e}_z (T^*_{n+1} - 1) \quad (21)$$

$$div \vec{v}^*_{n+1} = 0 \quad (22)$$

$$\frac{T^*_{n+1} - T^*_n}{\delta\tau} + \vec{v}^*_{n+1} \cdot \vec{\nabla} T^*_{n+1} = \frac{1}{Pr} \Delta T^*_{n+1} \quad (23)$$

The numerical processing of the nonlinear term [11] of equation (1) is carried out as follows:

We are given a vector function \vec{w} defined on Ω and satisfying the boundary conditions below: Let \vec{v} be a solution of the system: The elliptical character of this system of equations ensures \vec{v} the existence and uniqueness of the solutions. The solution of this problem is a function of \vec{w} ($\vec{v} = f(\vec{w})$). Thus \vec{v}^*_{n+1} appears as the fixed point of the function f : $\vec{v}^*_{n+1} = f(\vec{v}^*_{n+1})$. To find the fixed point \vec{v}^*_{n+1} , we proceed as follows: We arbitrarily give ourselves $\vec{v}^*_{n+1,0}$; then knowing, $\vec{v}^*_{n+1,m}$ we calculate $\vec{v}^*_{n+1,m+1/2}, p^*_{n+1,m+1/2}$, and $T^*_{n+1,m+1}$ solution of the following system of equations (24).

$$\frac{\vec{v}^*_{n+1,m+1/2} - \vec{v}^*_{n+1,m}}{\delta\tau} - \frac{1}{Re} \Delta \vec{v}^*_{n+1,m+1/2} + (\vec{v}^*_{n+1,m+1/2} \cdot \vec{\nabla}) \vec{v}^*_{n+1,m+1/2} = -\vec{\nabla} p^*_{n+1} - Gr \vec{e}_y (T^*_{n+1} - 1) \quad (24 a)$$

$$div \vec{v}^*_{n+1,m+1/2} = 0 \quad (24 b)$$

$$\frac{T^*_{n+1,m+1} - T^*_{n+1,m}}{\delta\tau} + \vec{v}^*_{n+1,m+1/2} \cdot \vec{\nabla} T^*_{n+1,m+1} = \frac{1}{Pr} \Delta T^*_{n+1,m+1} \quad (24c)$$

With the boundary conditions:

$$. \vec{v}^* = 0 \text{ on the walls} \quad \partial\Omega = \Sigma_1 \cup \Sigma_2 \quad (25)$$

$$. T^* = T_0 \text{ on } \Sigma_2 \quad (26)$$

$$. \frac{\partial T^*}{\partial \nu} = \frac{\nu^2}{g\beta T_0 l^5} Gr \text{ on } \Sigma_1 \quad (27)$$

$$\text{Then we calculate } \vec{v}^*_{n+1,m+1} \text{ by:} \quad \vec{v}^*_{n+1,m+1} = \omega \vec{v}^*_{n+1,m+1/2} + (1 - \omega) \vec{v}^*_{n+1,m} \quad (28)$$

The relaxation parameter ω is used to optimize the speed of convergence.

For the numerical resolution of the system (33), the following Uzawa type method is proposed [12] :

We are given arbitrarily $p^{*(0)}_{n+1,m+1}$ and $T^{*(0)}_{n+1,m+1}$. Then knowing $p^{*(k)}_{n+1,m+1}$ and $T^{*(k)}_{n+1,m+1}$, we calculate $p^{*(k)}_{n+1,m+1}$, $\vec{v}^{*(k)}_{n+1,m+1/2}$, $p^{*(k+1)}_{n+1,m+1}$ and $T^{*(k+1)}_{n+1,m+1}$ solution of the following system of equations (29).

$$\frac{\vec{v}^*_{n+1,m+1/2} - \vec{v}^*_n}{\delta\tau} - \frac{1}{Re} \Delta \vec{v}^*_{n+1,m+1/2} + \left(\vec{v}^*_{n+1,m+1/2} \cdot \vec{\nabla} \right) \vec{v}^*_{n+1,m+1/2} = -\vec{\nabla} p^*_{n+1} - Gr \vec{e}_y (T^*_{n+1} - 1) \quad (29 \text{ a})$$

$$p^{*(k+1)}_{n+1,m+1} = p^{*(k)}_{n+1,m+1} - \zeta \vec{\nabla} \cdot \vec{v}^{*(k)}_{n+1,m+1/2} \quad (29 \text{ b})$$

$$\frac{T^{*(k+1)}_{n+1,m+1} - T^*_n}{\delta\tau} + \vec{v}^{*(k)}_{n+1,m+1/2} \cdot \vec{\nabla} T^{*(k+1)}_{n+1,m+1} = \frac{1}{Pr} \Delta T^{*(k+1)}_{n+1,m+1} \quad (29 \text{ c})$$

With the boundary conditions:

$$\vec{v}^* = 0 \text{ on the walls} \quad \partial\Omega = \Sigma_1 \cup \Sigma_2 \quad (30)$$

$$T^* = T_0 \text{ on } \Sigma_2 \quad (31)$$

$$\frac{\partial T^*}{\partial \nu} = \frac{\nu^2}{g \beta T_0 l^5} Gr \text{ on } \Sigma_1$$

III. RESULT AND DISCUSSION

A. Calculation Conditions

In the case of a greenhouse, the studied fluid is air. We present our results are relative to the physical properties of the air at the reference temperature $T_0 = 25^\circ C$ under a pressure of 1 atm., the Prandtl of which corresponds to these conditions is $Pr = 0,7$. We consider the form factor $FR = \frac{D}{h}$ which is the ratio of the diameter of the circular base D considered as the major axis of the ellipse and the height h which is the minor axis of the ellipse. We study in our case the very flattened shapes characterized by $FR = \frac{8}{1} = 8$ where $D = 8$ and $h = 1$; and curved corresponding to $FR = \frac{8}{3} = 2,66$ with $D = 8$ and $h = 3$.

For the simulations, we take a time step value $\delta\tau = 0,05$ which is sufficient to properly observe the temporal evolutions of the streamlines corresponding to the different form factors and the different Grashof numbers [3].

The heat exchange by natural convection along the ellipsoidal wall being in the laminar flow regime, it is assumed that a constant heat flux density Q applies outside the ellipsoidal wall.

The viscosity of air is low, the value of the Grashof number is between 10^5 and 10^7 which corresponds to the Prandtl number between 0,71 and 1,2. We have studied two cases such as: $FR = 8$ and $FR = 2.66$ by taking two Grashof numbers $Gr = 10^5$ and 10^7 (case taken for the study of dry air we observe then the effect of the local Grashoff number until about 10^9 beyond this value the flow becomes turbulent). We note that the effect of the Prandtl number is interesting in the laminar regime because [8]: if the Prandtl number is very large in front 1, the fluid easily diffuses its momentum with respect to the heat. On the other hand, when the Prandtl number is very small compared to 1, the thermal boundary layer is thicker than the kinematic layer which reflects the existence of an immobile fluid zone when the temperature is greater than T_{init} .

For reasons of symmetry, the studies are done on the height along the axis $(0, \vec{z})$, this direction follows the minor axis of the semi-ellipsoid of revolution. The study being two-dimensional and we have presented the evolutions of the streamlines. in the plane $(0, x, z)$,

B. Current Lines

To better analyze the shape study: we consider two different shapes, one is flattened and the other rounded. For each shape, different points are studied by varying the Grashof values. Since the regime is laminar [8], the heat transfer intensity is dominated by conduction at the onset, although the velocity field is different from zero; we are in the presence of a pseudo-conductive regime. We have curves representing the spatial temporal evolutions of the streamlines relative to the Grashof number and reported at a point on the axis of $(0, \vec{z})$, they correspond to the different form factors illustrated by Figure 3a and Figure 3b.

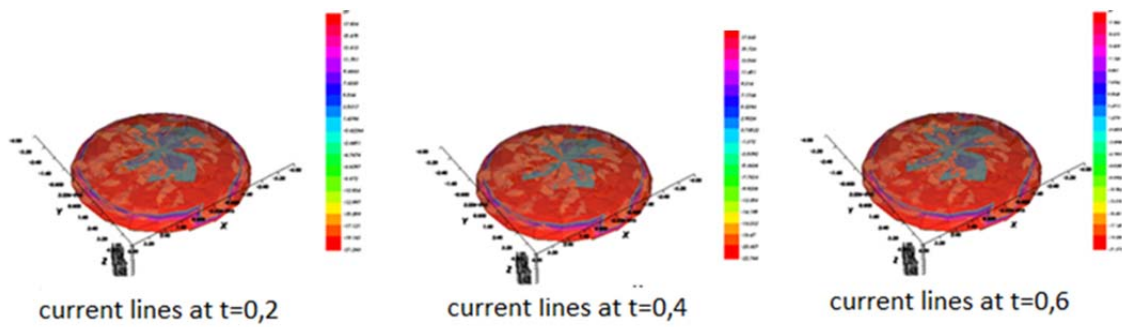


Figure3: a) Spatial evolution of streamlines under $Gr = 10^5$ and $FR = 8$

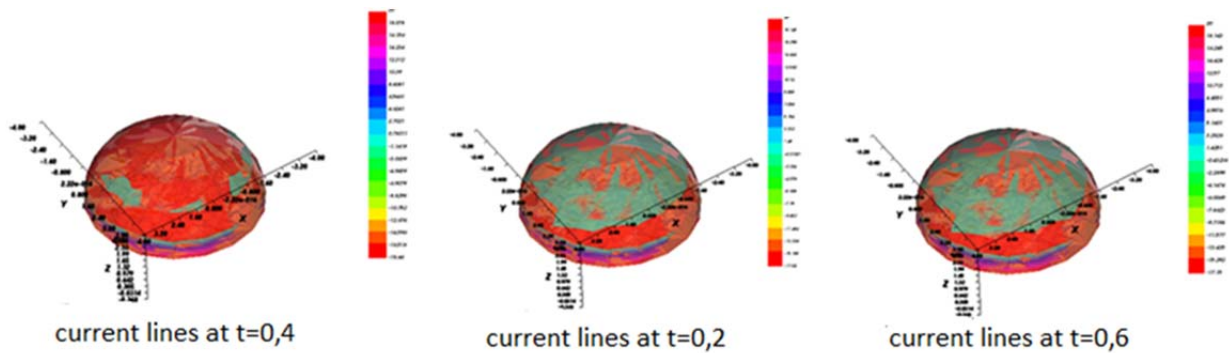


Figure3: b) Spatial evolution of streamlines under $Gr = 10^7$ and $FR = 2.66$

The analyzes on the behavioral evolutions of the convection currents are based on the studies of the influences of the various parameters among other geometry [4] or the form factor FR and the adimensional numbers such as number of Prandtl Pr , number of Grashof Gr , number of Nusselt Naked. We find that these numbers have the major effect on the allocation and distribution of thermal energy.

For both cases, the convective currents form on the base of the enclosure, since the enclosure is closed. They extend towards the corners and gradually meet along the wall. They form the convective currents

The analyzes on the behavioral evolutions of the convection currents are based on the studies of the influences of the various parameters among other geometry or the form factor FR , and the adimensional numbers such as number of Prandtl Pr , number of Grashof Gr , number of Nusselt Naked. We find that these numbers have the major effect on the allocation and distribution of thermal energy.

For both cases, the convective currents form on the base of the enclosure, since the enclosure is closed. They extend towards the corners and gradually meet along the wall. They form upward convective currents, and under the effect of gravitation, the fluid particles descend downwards (thermal mass effect or thermal inertia effect).

This phenomenon reproduces and regenerates the natural convection mechanism. This is due to the continuity equation (conservation of mass equation) [1]. It is important to know the physical behaviors of phenomena such as the change and variations of these convective currents. First, we presented the variations of convective currents as a function of the Grashof number. In its physical sense, this number quantifies the importance of the forces of Archimedes compared to the viscous forces which is the force of viscosity of the fluid, therefore to check the movement of the air in the enclosure.

We then realize that there is a zone of concentration of convection current.

The analysis relates to the knowledge of the points and the geometric locus that are particularly significant for the aerothermal parameters (very hot zone, or current zone at maximum speed). Taking into account the Prandtl number which defines the

relationship between the momentum diffusivity (Navier-Stokes equation) and the thermal diffusivity (Fourier equation), it characterizes the velocity distribution with respect to the temperature distribution [13].

This number is practically chosen for the studied fluid (in our case it is air). The Nusselt number characterizes the transfer between the heated wall and the moving fluid. This study therefore leads to the determination of the average Nusselt number which represents the importance of the convective effect compared to the conductive effect. We have presented in Figure 4a and Figure 4b some temporal evolutions of convective currents.

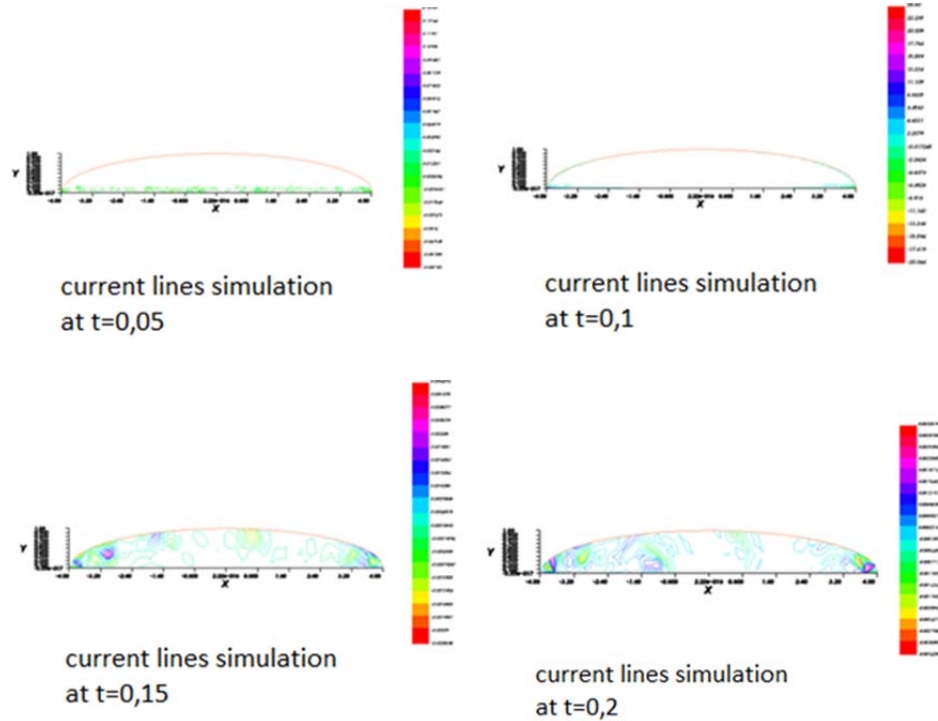
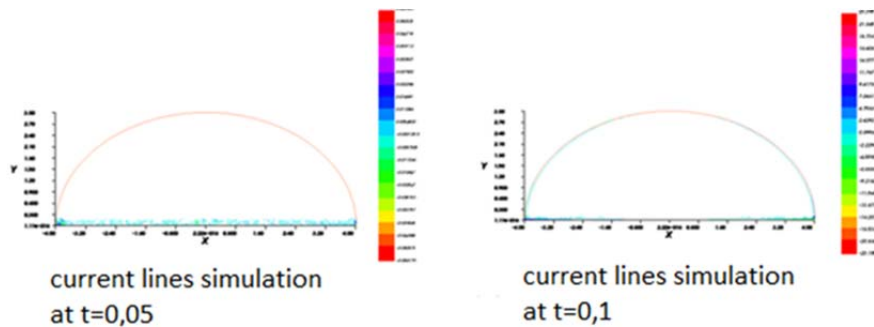
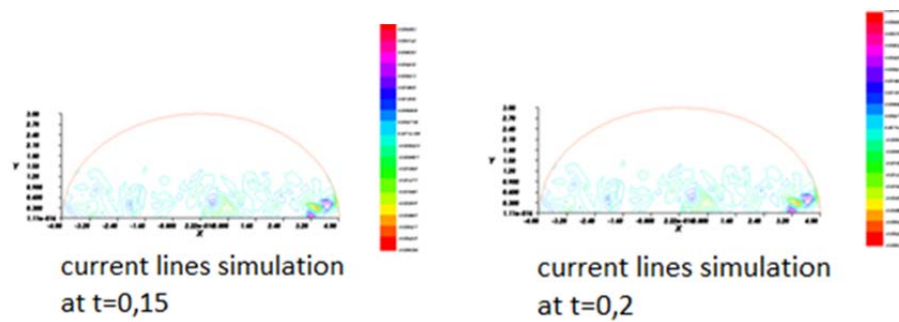


Figure 4: a) Time evolution of convective currents for $FR = 8$ with $Gr = 10^5$



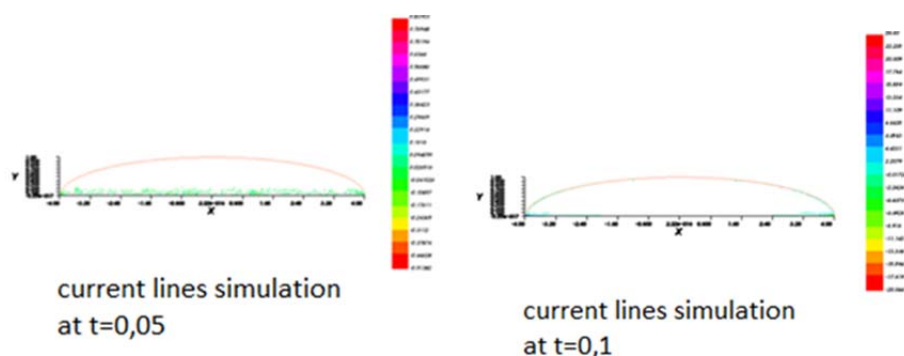

 Figure 4: b) Time evolution of convective currents for $FR = 2.66$ with $Gr = 10^5$

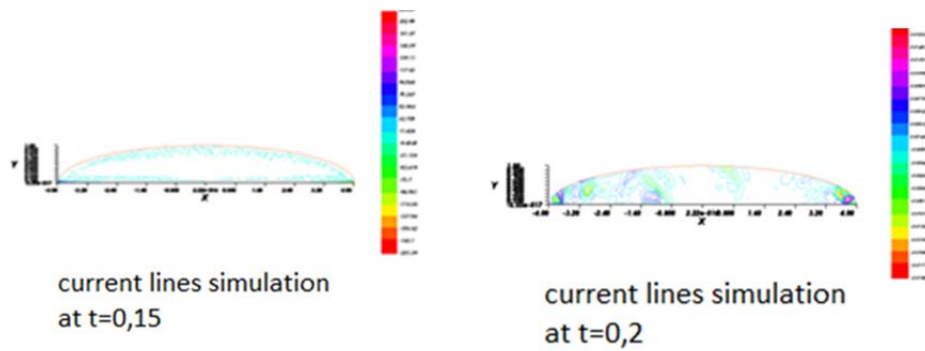
By taking another value of the higher Grashof number $Gr = 10^7$, we obtained the evolutions of the following convective currents by still considering the same form factors as the previous ones. The convective currents are transformed into current lines and their evolutions according to the time step are represented by Figures 3.

For the shape factor $FR = 8$ with the Grashof number $Gr = 10^5$ and $Gr = 10^7$ the streamlines vary little at the beginning of the time steps, then they stabilize while keeping constant paces. This phenomenon reflects the preponderance of conduction because the temperature increases rapidly. It keeps a constant value so there is permanent heating inside the enclosure because the lines of currents remain almost immobile as represented by the speed variation curve (heating). Convection occurs because streamlines vary in space. It is found that the height predominates on the creation of the movement of the natural convection because the streamlines disperse in all the surfaces and their variation is a function of the geometry of the enclosure.

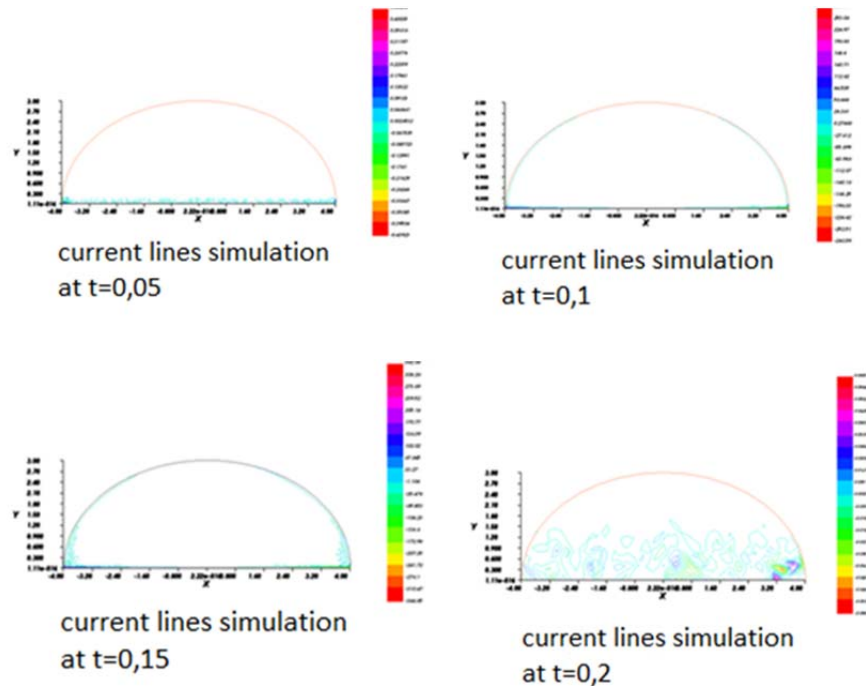
The presence of the constant density heat flux heats [7] the wall on the outside, this results in the variation of the speed of the fluid particles to create the speed gradient. The flow of ascending air convection currents (hot current) appears to the variation of this velocity gradient which carries the fluid particles to all points of space. Under the effect of the variation of the heat applied to the outside, the density varies when there is a rise in temperature. Particles move with different velocities that vary over time.

This value changes from the minimum value to the maximum value when the temperature gradient varies inside the closed enclosure. The temperature varies according to the direction of the ascending height, up to a maximum value (the peak value which reflects the steep slope of the curve because there is a strong rise in value until reaching the maximum value: dryer operation [14]) illustrated by the Figure 4a; and under the effect of gravity, they descend while cooling and reach the lower part of the containment (cold part). The regenerating movement creates the natural convection mechanism; it then reigns inside the wall. The velocities at three different points along the height (at the point (0,0.25), at the point (0,0.5) and at the point (0,0.75)) under a Grashof number $Gr = 10^5$ are plotted by the Figure 5a




 Figure 5: a) Time evolution of convective currents for $FR = 8$ with $Gr = 10^7$

For the case of $FR = 2,66$ (sous $Gr = 10^5$ et $Gr = 10^7$) the streamlines present variations at the beginning and at the end of the studied time steps. They keep a constant pace in a few time steps (period of circulation is maximum on the surface areas Figure 5b)


 Figure 5: b) Time evolution of convective currents $FR = 2.66$ with $Gr = 10^7$

C. Velocity And Temperature

For the case of the flattened shape, we found that the convective currents form on the base of the surface. They are gradually distributed on the corners and disperse over the entire surface of the wall. As for the heat exchange that appears between the fluid and the heated wall, the break in thermodynamic equilibrium causes variations in the parameters including temperature and velocity over time. This variation is a function of the geometry of the enclosure. The presence of the constant density heat flux heats the wall on the outside, this results in the variation of the speed of the fluid particles to create the speed gradient.

The flow of ascending air convection currents (hot current) appears to the variation of this velocity gradient which carries the fluid particles to all points of space. Under the effect of the variation of the heat applied to the outside, the density varies when there is a rise in temperature. The particles move with different velocities that vary over time. This value changes from the minimum value to the maximum value when the temperature gradient varies inside the closed enclosure.

The temperature varies according to the direction of the ascending height, up to a maximum value (the peak value which reflects the steep slope of the curve because there is a strong rise in value until reaching the maximum value) illustrated by the Figure 5; and under the effect of gravity, they descend while cooling and reach the lower part of the containment (cold part). The regenerating movement creates the natural convection mechanism; it then reigns inside the wall. The velocities at three different points along the height (at the point (0,0.25), at the point (0,0.5) and at the point (0,0.75)) under a Grashof number $Gr = 10^5$ are plotted by the Figure 6

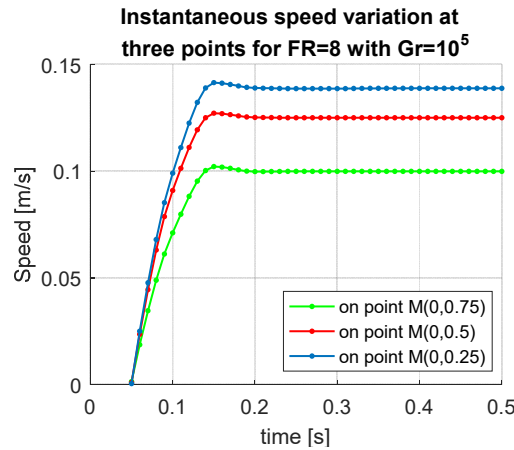


Figure 6: temporal variation of the flow velocity for $FR = 8$ and $Gr = 10^5$

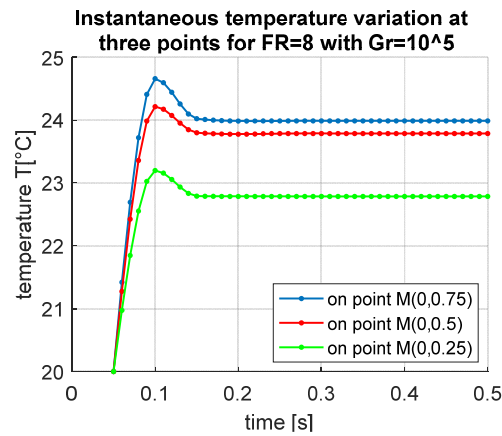
The curves presented below show that the speed increases when approaching the wall because the more heated fluid particles are lighter so they move faster, moving away from the wall (coordinates of the points higher than compared in the middle of the height) along the minor axis of the semi-ellipsoid, the temperature decreases because the fluid particles cool when approaching the base, they have lower velocity. We can admit that the appearance of the phenomenon of conduction [6] happens in the vicinity of the wall, more precisely by approaching the upper part of the middle of the height while the formation of convection currents takes place on the lower part.

The curves of temporal variations of the temperature appear with a peak of value. This value shows that there is a part of the air which warms up enormously compared to the others. Part of the fluid is located in the vicinity of the wall so it heats up more, then the heat exchange modifies the thermodynamic equilibrium in the enclosure, the temperature will stabilize until the state of equilibrium illustrated is obtained by Figure 7. We have the temperatures at three different points according to the height (at the point (0,0.1), at the point (0,0.5) and at the point (0,0.75)) under a Grashof number $Gr = 10^7$

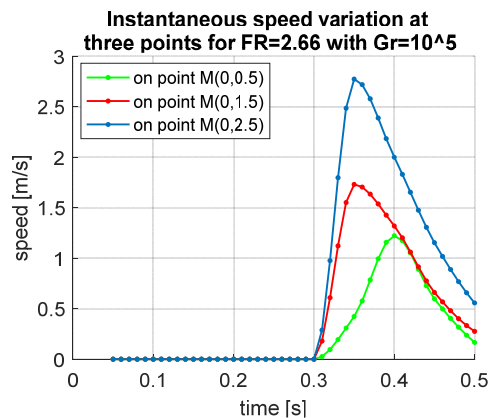
The velocity and temperature variation curves have almost the same shapes for the form factor $FR = 8$.

The analysis is based on studies of the speed and temperature curves at 3 different points depending on the height. On the surface, they maintain an increasing pace on these three points of study.

The point M (0,0.5) is taken as a reference, below this point is the point M (0,0.25) where the two parameters have lower values because the fluid particles are still cooled so they move at low speed, and above this point where the point M(0,0.75) is located, the speed increases with the rise in temperature, then they will be zero. In addition, we studied the curves representing the variations of the thermoconvective parameters in the case of the domed shape (the speed and the temperature are a function of the dimensionless numbers).


 Figure 7: Temporal variation of temperature for $FR = 8$ and $Gr = 10^5$

Passing through the form factor $FR = 2.66$ the velocity is almost zero during a time interval, it increases abruptly to a maximum value and then it drops to a constant value to stabilize. This reflects the effect of enclosure height because the convection current took a long time to reach the top of the enclosure. The velocities at three different points at point (0.0.5), point (0.1.5) and point (0.2.5) are shown in Figure 8.


 Figure 8: Temporal variation of flow velocity for $FR = 2.66$ and $Gr = 10^7$

Indeed, the fluid particles swirl before arriving on the cold part at the bottom. The cooling time is slower before warming up and reaching the upper part of the wall. During the convective cycle, the speed of the fluid particles is relative to the Grashof number which depends on the viscosity (knowing that air is a viscous fluid). Because of the friction in contact with the wall, the viscosity decreases when the Grashof number increases. We take into account that the viscosity is a function of the temperature, it decreases when the temperature increases. The shape of the temperature variation curve (before stabilizing) is therefore increasing because it is relative to the increase in the Grashof number. That of the speed curve which increases with temperature. The Grashof number is a determining parameter for the flow of air in the enclosure because it justifies the effect of viscosity (as a function of temperature) during the flow of a fluid. This number reacts on the formation of convection currents under the effect of the variation of the temperature with the form factor. The evolution of the temperature depends relatively on the variation of the speed according to the transfer zone, in particular in the vicinity of the axis where the heat exchange zone is more intense than represented in Figure 9. We have the temperatures at three different points at point (0.0.5), point (0.1.5) and point (0.2.5).

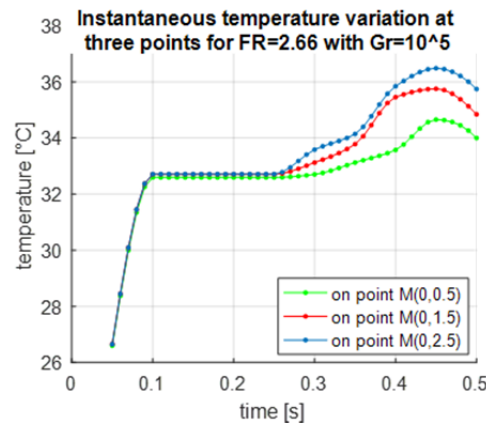


Figure 9: Temporal variation of temperature for $FR = 2.66$ and $Gr = 10^7$

In any case, the values of the thermoconvective parameters vary mainly according to the form factor. This parameter is apparently dominant than the others, we subsequently find the variations of the curves drawn at the same Grashof number under the different form factors, then of the curves presented the same form factor but at the different Grashof number. Moreover, in the case of a lower form factor, it keeps a value almost zero until a certain time step then it increases sharply to reach a peak value, it decreases slowly to stabilize [15].

For the case of $FR = 8$ the slope of the temperature variation curves is gentle because the wall heats up quickly, the heat exchange between the fluid and the wall takes place quickly, so the air is almost always heated in the enclosure, the convection did not take place facing the conduction, geometrically the path of circulation of the fluids is less long then they flow quickly while holding in the heated state. On the other hand, for $FR = 2.66$ the temperature rises slowly (steep slope for the temperature variation) before stabilizing at such a value [2]; on the other hand the speed is with the gentle slope because the flow is slower consequence of the high height the path of circulation of the fluids is longer therefore the heat exchange is slow. In this case the variation of the temperature in the chamber is almost stable while remaining constant over time.

D. Nusselt Numbers

The figure represents the temporal evolution of the global Nusselt number for different form factors ($FR = 8$ and $FR = 2.66$) as a function of the Grashof numbers ($Gr = 10^5$ and $Gr = 10^7$), the work focuses on the calculations of the average Nusselt number by studying the temperature distributions (across the surface) from the base to the top.

The presence of thermal mass (or thermal inertia) created by the heat flux of constant density applied to the wall involves the mechanism of natural convection. The Nusselt number highlights the comparison of the conductive effect with the convective effect at any point of the domain considered according to the geometric shape studied. It also justifies the importance of convection compared to conduction because this number represents the gradual variation (or gradient) of the temperature along the direction of the height. This temperature gradient indicates the plots of the isotherms in the system under consideration. In order to know the physical meaning of the Nusselt number Nu , we present the comparative curves under different cases such as different shape factor at the same Grashof number and that of the same shape factor under different Grashof number to deduce the physical meaning of the Nusselt number Nu . onset of conduction and convection in the enclosure. Two cases of comparison are taken into account, including:

- . A form factor with different Grashof numbers (Table 1)

The comparative study highlights the effect of viscosity for the movements of convective currents in the containment. This case characterizes the formation of streamlines as well as the distribution of velocities and temperatures which is due to the effect of viscosity. The variations of the Nusselt number from a form factor with different Grashof numbers are plotted by a curve. In the case of the flattened shape, by comparing the two curves with the same form factor $FR = 8$ under different Grashof numbers $Gr = 10^5$ and $Gr = 10^7$, the Nusselt numbers are of the same shape increasing, they are separated from each other with a certain value according to the time step, then they reach almost the same peak values " $Nu = 8,67$ and $Nu = 9,41$ " under a very short space of time. This indicates the absence of the convection phenomenon, apparently conduction dominates (Table). Case of the

curved shape, the comparison of these two curves shows that they have an increasing variation, the Nusselt number values deviate from each other at a high peak value " $Nu = 28,63$ and $Nu = 57,47$ ", this difference in value is an indication of the existence of the convection phenomenon. Other curves represent the variations of the Nusselt number in the case of the same Grashof number but for different form factors.

. Different form factors with Grashof number (Table 1)

This comparison shows the distribution of currents in the enclosure. The fluid circulations do not seem the same for the different geometries. The variations in speeds and temperatures are distributed under the effect of the geometry. For the variations of the Nusselt number from different form factors at the same Grashof number, they are represented by a curve. On the same graph, Figure 10 illustrates the curves of comparative variation of the Nusselt numbers in the case where the different shape factors under the same Grashof number.

Table 1: NUSSOLT NUMBER VALUE CORRESPONDING TO THE DIFFERENT GRASHOF NUMBER RELATIVE TO THE DIFFERENT SHAPE FACTOR

Form factor FR	Nusselt number Nu	
	$Gr = 10^5$	$Gr = 10^7$
FR=8	8,67	9,41
FR=2,66	28,63	57,47

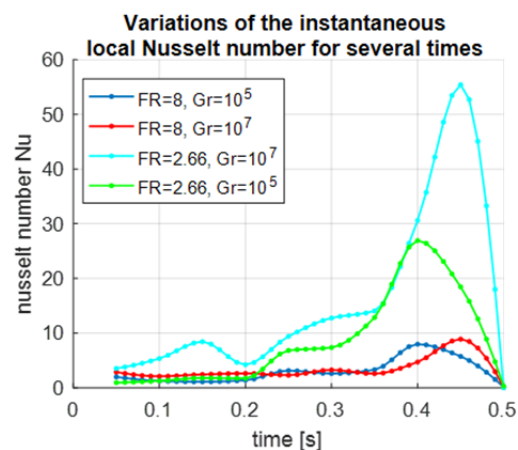
According to the speed and temperature curves obtained, the flat wall (approximate surface of the very flattened ellipsoid) heats up rapidly compared to the curved surface, we have an average peak value of the velocity as a function of the time step $v = 0,12 \text{ m.s}^{-1}$ for the flattened surface (Figure 6) and $v = 1,75 \text{ m.s}^{-1}$ for the curved surface (Figure 8). These values show that the fluid particles moving in the vicinity of the wall for the flat shape with temperature value $T = 24,3^\circ\text{C}$, they are lower compared to the average peak value in the case of the curved shape with temperature value $T = 34,2^\circ\text{C}$ because the recirculation of the fluid particles in the enclosure is low.

While for the case of the curved surface, the fluid particles admit a high speed because their circulation in the chamber is ensured by the mechanism of natural convection, they keep a constant value thanks to the faster heating of the wall.

For a flat surface which is close to the very flattened ellipsoidal shape, the Nusselt number as a function of the time step is very low compared to the curved structure (very high Nusselt number, Figure 10), plus the curvature of the wall is high, the Nusselt number increases, resulting in better convection in the enclosure (Table 2).

Table 2: NUSSELT NUMBER, TEMPERATURE and VELOCITY VALUE CORRESPONDING TO THE DIFFERENT GRASHOF NUMBER RELATIVE TO THE DIFFERENT SHAPE FACTOR

Form factor FR	Temperature T [°C]	velocity v[m/s]	Nusselt number Nu	
			$Gr = 10^5$	$Gr = 10^7$
FR=8	24,3	0,12	8,67	9,41
FR=2,66	34,2	1,75	28,63	57,47


 Figure10: Nusselt number variation for $FR = 8$ under $Gr = 10^5$; $FR = 8$ under $Gr = 10^7$ compared with $FR = 2.66$ under $Gr = 10^5$; $FR = 2.66$ under $Gr = 10^7$

IV. CONCLUSION

In this report, a new type of geometry that highlight conditions which ensure a laminar natural convection is studied and analyzed. To do this, we studied the nature of the thermoconvective movements developing within a fluid medium limited by a semi-ellipsoid of revolution with a circular base, in terms of heat transfers induced by each form of flow. For this purpose, the Navier-Stokes equations, the continuity equation and the Fourier equation is solved by the use or finite element method combined with Uzawa type method.

We considered the effect of the shape factor of the elliptical wall and the Grashof number on the results obtained in the form of streamlines, and the average Nusselt number. Result shows that the geometric shape constitutes one of the technical requirement during the construction of a structure. In fact, laminar convection actually exists in a domed structure. It is recommended for a greenhouse to opt for a domed shape to improve the yield of a cropping system. Thus the half-ellipsoid shape responds well to this requirement.

REFERENCES

- [1] Y.S. Tian et T.G. Karayiannis, Low turbulence natural convection in an air filled square cavity Part I: the thermal and fluid

- flow fields, Int J.of Heat and Mass Tr., 849-866 (2000).
- [2] Jain D, Modeling the performance of greenhouse with packed bed thermal storage on crop drying application, Journal of Food Engineering, 71 (2005) 170-178
- [3] Lin YS, Akins RG. Thermal description of pseudo-steady-state natural convection inside a vertical cylinder. Int J Heat Mass Transfer 29, 301-307 (1986).
- [4] Patterson J, Imberger J. Unsteady natural convection in a rectangular cavity. J Fluid Mech 100, 65-86 (1980).
- [5] J. FAUVEAU Convection naturelle dans une couche poreuse limitée par deux surfaces sphériques concentriques. Thèse de doctorat de troisième cycle, Université de Bordeaux I, 1979.
- [6] Willit D.H., Chandra P. et Peet M.M., Modelling solar Energy Storage Systems for Greenhouses, Journal of Agricultural Engineering Research, 32 (1985) 73-93.
- [7] M. Djezzar, A. Chaker, and M. Daguénet, Numerical study of bidimensional steady natural convection in a space annulus between two elliptic confocal ducts. Influence of internal eccentricity. Revue des Energies Renouvelables, Volume 8, Numéro 1, Juin 2005.
- [8] S. PATANKAR. Numerical heat transfer and fluid flow 0 Edition Energoatomizdat, Moscou 1984.
- [9] YOGESH JALURIA. Natural convection heat and mass transfer. Edition Mir, Moscou, 1983.
- [10] L. LANDAU et E. LIFCHITZ. Mécanique des fluides. Edition Mir, Moscou, 1971.
- [11] M. FORTIN, R. GLOWINSKI. « Méthodes de Lagrangien augmenté : application à la résolution numérique des problèmes aux limites ». Bordas Paris 1992.. Edition Mir, Moscou, 1971.
- [12] P.G CIARLET « Introduction à l'analyse numérique matricielle et à l'optimisation » Masson Paris 1990.
- [13] E. F. NOGOTOV. Applications of numerical heat transfer. Mc Graw Hill Book Company, New York, 1978.
- [14] M. Daguénet, 'Les Séchoirs Solaires, Théorie et Pratique', U.N.E.S.C.O, 1984.
- [15] Nishina H. et Takakura T., Greenhouse heating by means of latent heat storage units, Acta Hort (Energy in Protected Cultivation III), 148 (1984) 751-754.